11652 *J. Phys. Chem. A* **2007,** *111,* 11652−11660

Atmospheric Oxidation Mechanism of Bromoethane

Mónica Martínez-Avilés, Claudette M. Rosado-Reyes, and Joseph S. Francisco*

Department of Chemistry and Department of Earth and Atmospheric Sciences, Purdue University, West Lafayette, Indiana 47907

Received: May 18, 2007; In Final Form: August 13, 2007

A mechanism for the atmospheric oxidation of bromoethane is proposed from an ab initio study. Using CCSD(T)/6-311++G(2df,2p)//MP2/6-31G(d) level of theory, the structure and energetics of the 35 species and transition states involved in the atmospheric oxidation of bromoethane are examined. From these calculations, reaction enthalpies and activation energies to characterize the potential energy surface of the proposed mechanism for the complete atmospheric degradation of bromoethane are determined. The studies revealed that the hydrogen abstraction from the α carbon has the lowest activation energy barrier of all the possible abstractions, making this pathway the most energetically favored pathway for the atmospheric oxidation process. The brominated species that result from the oxidation at the α carbon are $BrC(O)CH_3$ and $BrC(O)H$. Other species resulting from oxidation initiated at the β carbon are also identified.

1. Introduction

Several chlorofluorocarbons (CFCs) and halocarbons are in need of replacements as part of the agreements of the Montreal Protocol on Substances that Deplete the Ozone Layer.[1,2] A number of the replacements that have been proposed are considered very short-lived (VSL) substances, since their chemical lifetimes are similar to tropospheric transport time scales. Characteristically, the concentrations of VSL halogen source gases proceed from natural sources and range in a few parts per thousand for Br.[3,4] Brominated compounds in the vapor phase are released into the troposphere, where they are transported to the stratosphere, producing Br atoms that catalyze ozone destruction 40−50 times more effectively than Cl atoms.[5−9] There are several atmospheric processes that affect the transport of the halogen to the stratosphere (i.e., physical and dynamical processes). Due to the complexity of these processes, it has not been easy to estimate the impact of VSL halogen source gases on stratospheric ozone.[3] Intermediate degradation products and their respective degradation pathways play an important role, as well. Typically, the expected degradation products are readily converted to inorganic halogen by further reacting with scavengers present in the atmosphere.

The main use of bromoethane, also known as alkyl bromide, is as an ethylating agent in chemical synthesis.[10] This brominated alkane is also used as a refrigerant, a fumigant, and as a component of gasoline.[10,11] As a natural source, Class and co-workers[11] found bromoethane to be a minor component of brominated and bromochlorinated methanes released to the surrounding air from brown algae in the North and South Atlantic. As well, Greenberg and co-workers,[12] in collaboration with the Martin Ryan Institute, detected bromoethane and other marine organic halides near Mace Head, Ireland. Another study performed over the Pacific Ocean between California and New Zealand showed a median concentration of bromoethane of 0.3 ppt.[13] This value is in agreement with the ones reported by Carpenter and co-workers.[14] Another source of bromoethane is volcanic emissions. Bromoethane was part of the organohalogenated compounds detected in fumaroles and lava gas by a research team led by scientists from the Max-Plank-Institute for Aeronomy.[15] Bromoethane has also been detected in air samples collected near chemical manufacturing areas. A bromoethane concentration of 170 mg/L has been reported for municipal landfill leachate that had been treated with chlorine.[16,17]

On the basis of its vapor pressure, bromoethane exists entirely in the vapor phase in the atmosphere. The Henry's law constant for bromoethane has been estimated to be 0.76 kPa$\cdot$m^3/mol. This highlights the importance of volatilization from environmental waters. If discharged into water, the removal mechanism of bromoethane is hydrolysis and volatilization. If bromoethane is released to soil, hydrolysis will play a major role under wet soil conditions.

For many natural and anthropogenic gases, reaction with the hydroxyl radical (OH) is considered the most effective fate in order to clean the atmosphere of any possible build-up of toxic atmospheric gases contributing to the greenhouse effect.[3,18−24] Experimentally, kinetic studies have been performed to study the rate of reaction of bromoethane with an OH scavenger.[25−28] Having an estimated rate of reaction of 0.334×10^{-12} cm^3/molecule per second, bromoethane is expected to have a slow atmospheric degradation due to its reaction with hydroxyl radicals.[21,29] This value corresponds to a half-life of ~48 days at an atmospheric concentration of 5×10^5 hydroxyl radicals/cm^3. Donaghy and co-workers[28] determined by experimental means that the atmospheric lifetimes for bromoethane and its respective reactions with hydroxyl radicals and chlorine were 51−73 days and 1.2 years, respectively. When modeling the atmospheric impact of compounds similar to bromoethane, a challenge is to determine its ability to detect the concentration of ozone in the stratosphere. One of the most important factors that need to be determined is the actual amount of bromoethane and its reaction products that carry bromine into the stratosphere and, by means of the Br released, determine the ozone destroyed by the bromine.

The degradation mechanism of bromoethane is initiated via its reaction with OH. There are two possible pathways that the reaction can undergo leading to the formation of different degradation products: α and β H-abstraction. For purposes of

10.1021/jp073862w CCC: $37.00

clarity, the halogenated carbon is called the α carbon, and the adjacent carbon is referred to as the β carbon. These possible pathways and their resultant radicals are shown in reactions 1a and 1b.

$$BrCH_2CH_3 + OH \xrightarrow{\alpha} BrCHCH_3 + H_2O \quad (1a)$$

$$\xrightarrow{\beta} BrCH_2CH_2 + H_2O \quad (1b)$$

The radical species produced are readily converted to more stable substances via subsequent reaction with O_2. Once the organic peroxy radicals (RO_2) are formed, the degradation continues via reaction with nitric oxide (NO), where it is converted to NO_2 and the alkoxy radical (RO). The alkoxy radical can either further react with O_2 or undergo spontaneous fragmentation to continue the atmospheric degradation of bromoethane through the degradation of its intermediate degradation products. The yield of the degradation products depends on the concentration of the scavengers (i.e., OH, O_2, and NO) and the atmospheric conditions.

Natural and anthropogenic processes produce the partially halogenated compounds that are present in the atmosphere.[30] The atmospheric oxidation process of these compounds has been of interest.[31−49] Even though data on the chemistry of α-brominated alkoxy radicals have been available,[31,35,48] not until Orlando and co-workers[30] studied bromoethane have the atmospheric conditions been taken into account to understand the degradation mechanism for bromoethane. With the aim of identifying other brominated species not yet accounted for, in this study, we present a complete degradation mechanism for the atmospheric oxidation of bromoethane.

2. Computational Methods

The Gaussian 03 suite of programs are used to perform all the calculations discussed in this article.[50] The geometries of the molecules comprising the complete degradation mechanism for the atmospheric oxidation of bromoethane are fully optimized, and their frequencies were obtained with the second-order Møller-Plesset (MP2) perturbation method.[51] These frequency calculations provided all the thermochemical data and vibrational frequencies of all the species involved in the mechanism under study. True transition state structures are characterized by one imaginary frequency. The MP2-optimized geometries are used in a series of single-point energy calculations involving the following two levels of theory and basis set combinations: CCSD(T)/6-311G(2d,2p) and CCSD(T)/6-311++G(2df,2p). To obtain the total energies of the various species, the calculated energies are corrected by using the ZPE obtained at the MP2 level. Zero-point energy (ZPE) corrections are added to the final predicted energetics to account for the effects of molecular vibrations persisting at 0 K. These total predicted energies are then used to determine the enthalpies of the reactions (ΔH_r), as well as the activation energy (E_a) barriers involved in the mechanism under study.

3. Results and Discussions

3.1. Reaction Pathways in the Atmospheric Degradation of Bromoethane. *3.1.1. Structures of the Species Involved in the Atmospheric Degradation of Bromoethane.* There are two different hydrogen environments in bromoethane, as observed in Figure 2a. The first H abstraction is obtained by the reaction of bromoethane with the OH scavenger at the α carbon. This reaction generates a radical center on the halogenated carbon, BrCHCH$_3$ (Figure 2b). Changes in the structure of the parent molecule are noticeable when compared to the radical formed by the H abstraction. The one hydrogen on the halogenated carbon has a bond length of 1.082 Å, and the C−Br bond length decreases to 1.882 Å. In addition, the $C_\alpha-C_\beta$ bond decreases from 1.513 to 1.485 Å as the radical is formed. This radical is readily converted into a peroxy radical via its reaction with O_2, $BrCHO_2CH_3$ (Figure 2c). The peroxy radical reacts with NO to form $BrCHOCH_3$ (Figure 2d). This newly formed radical has a C−Br bond length of 2.006 Å and a C−O bond with length of 1.346 Å. The reduced radical stabilizes in three separate ways, dividing the pathway into three pathways. One pathway is the spontaneous fragmentation of $BrCHOCH_3$ to form Br plus HC(O)CH$_3$. The final product of this dissociation, HC(O)CH$_3$, has a CO bond of 1.222 Å and a C−C−O angle of 124.3°, as shown in Figure 2e. Alternatively, there is another dissociation route that forms CH_3 and BrC(O)H (Figure 2f). As observed in Figure 2f, this brominated aldehyde has a CO bond of 1.195 Å and a C−Br bond length of 1.960 Å. When the methyl radical reacts with an O_2 molecule, it forms CH_3O_2 (Figure 2g). The peroxy radical undergoes a reduction as it reacts with NO to form CH_3O (Figure 2h). Once again, an O_2 molecule oxidizes this newly formed alkoxy radical to form HC(O)H (Figure 2i). Formaldehyde is a symmetric molecule with a CO bond length of 1.220 Å and H−C−O angles of 122.2°. On the other hand, a reaction among the alkoxy radical and O_2 can take place, forming HO_2 and BrC(O)CH$_3$ (Figure 2j). This reaction causes the CO bond to be shortened to 1.194 Å and the C−C−O angle to increase to 128.9°. The C−Br length is 2.002 Å and the angle between Br−C−O is 120.5°.

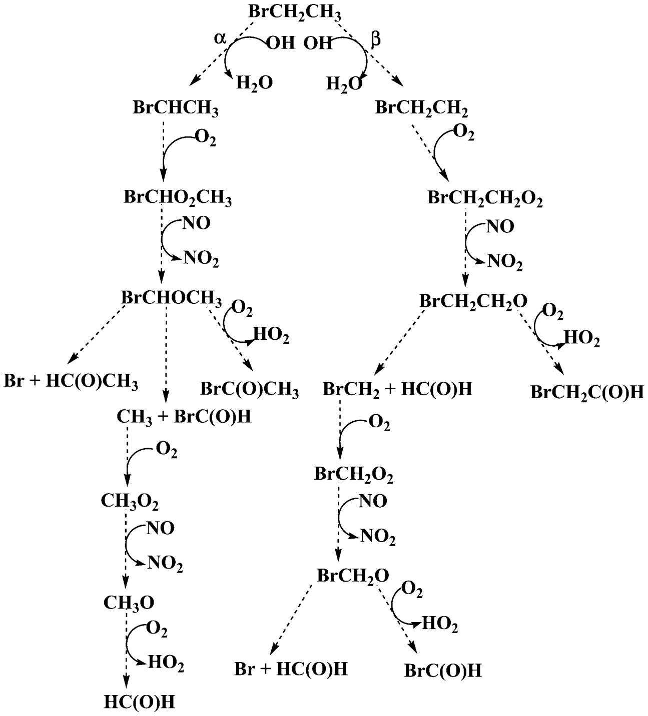

Figure 1. Atmospheric degradation pathways of bromoethane.

The second pathway involves an OH molecule that can abstract an H from the carbon β to the bromine. This β abstraction leads to $BrCH_2CH_2$ (Figure 2k). This radical differs from its parent molecule in that the $C_\alpha-C_\beta$ changes from 1.513 to 1.462 Å. In addition, the hydrogen in the β carbon decreased its length to 1.096 Å. This radical can readily be oxidized by O_2 forming $BrCH_2CH_2O_2$ (Figure 2l). This newly formed peroxy radical can also be reduced by NO to form $BrCH_2CH_2O$ (Figure

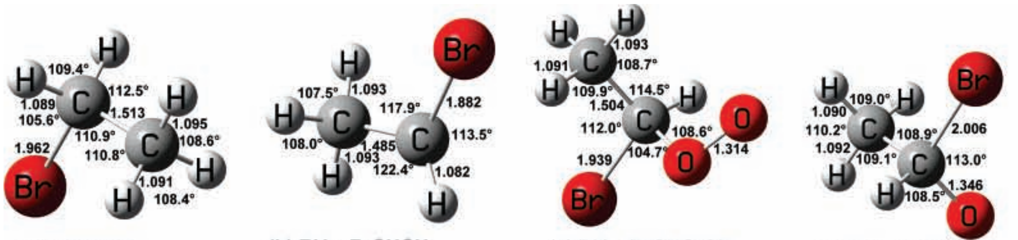

(a) $BrCH_2CH_3$ (b) $RI1_a$: $BrCHCH_3$ (c) $RI1_b$: $BrCHO_2CH_3$ (d) $RI1_c$: $BrCHOCH_3$

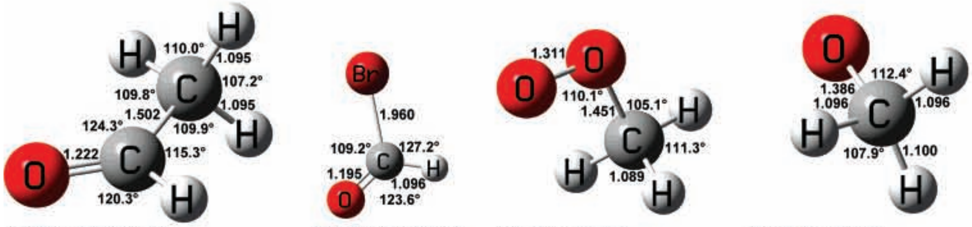

(e) $P1_a$: $HC(O)CH_3$ (f) $P1_b$: $BrC(O)H$ (g) $RI1_d$: CH_3O_2 (h) $RI1_e$: CH_3O

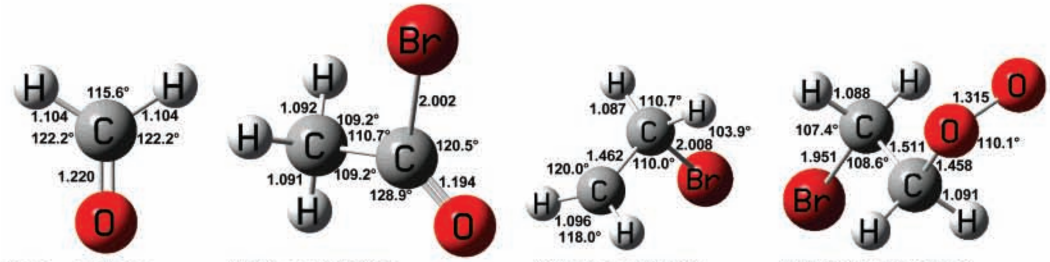

(i) $P1_c$: $HC(O)H$ (j) $P1_d$: $BrC(O)CH_3$ (k) $RI2_a$: $BrCH_2CH_2$ (l) $RI2_b$: $BrCH_2CH_2O_2$

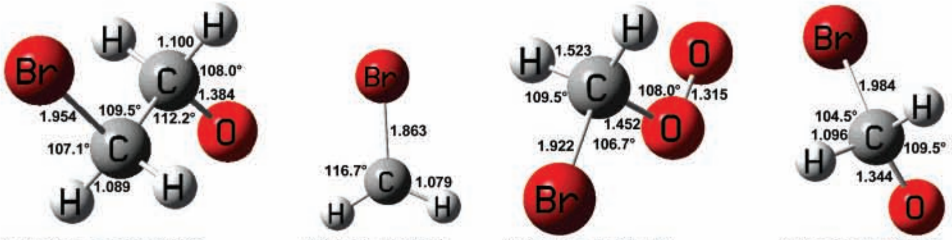

(m) $RI2_c$: $BrCH_2CH_2O$ (n) $RI2_d$: $BrCH_2$ (o) $RI2_e$: $BrCH_2O_2$ (p) $RI2_f$: $BrCH_2O$

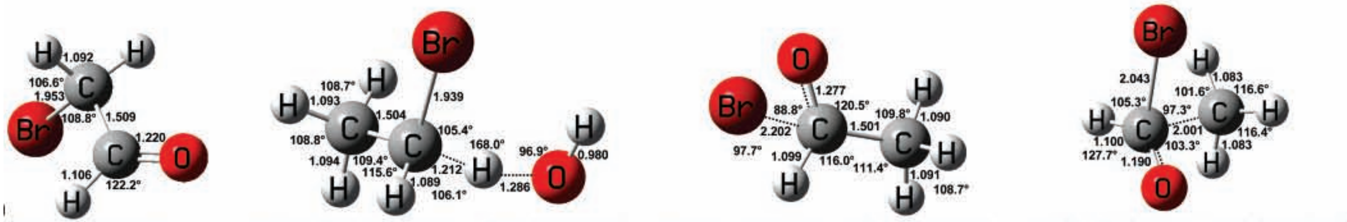

(q) $P2_a$: $BrCH_2C(O)H$ (r) $TS1_a$: $[BrCH_2CH3 + OH \rightarrow BrCHCH_3 + H_2O]^‡$ (s) $TS1_b$: $[BrCHOCH_3 \rightarrow Br + HC(O)CH_3]^‡$ (t) $TS1_c$: $[BrCHOCH_3 \rightarrow BrC(O)H + CH_3]^‡$

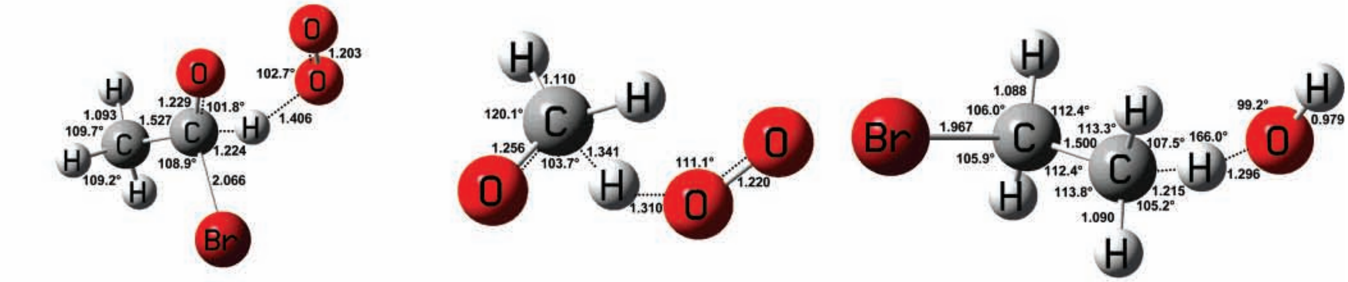

(u) $TS1_d$: $[BrCHOCH_3 + O_2 \rightarrow BrC(O)CH_3 + HO_2]$ (v) $TS1_e$: $[CH_3O + O_2 \rightarrow HC(O)H + HO_2]^‡$ (w) $TS2_a$: $[BrCH_2CH_3 + OH \rightarrow BrCH_2CH_2 + H_2O]^‡$

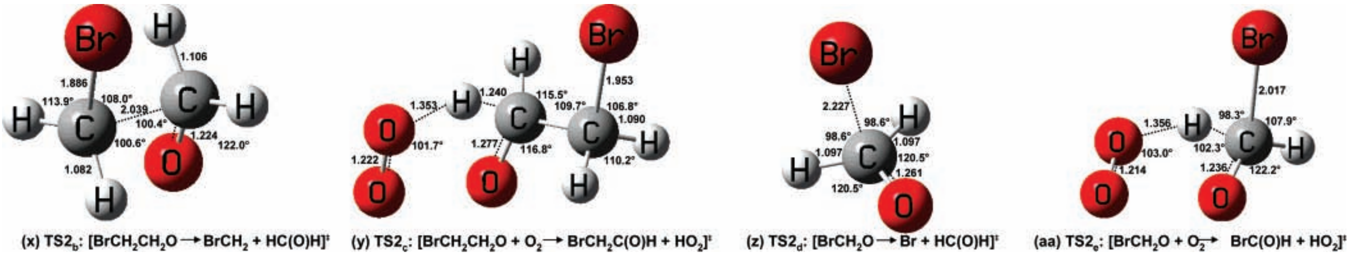

(x) $TS2_b$: $[BrCH_2CH_2O \rightarrow BrCH_2 + HC(O)H]^{\ddagger}$ (y) $TS2_c$: $[BrCH_2CH_2O + O_2 \rightarrow BrCH_2C(O)H + HO_2]^{\ddagger}$ (z) $TS2_d$: $[BrCH_2O \rightarrow Br + HC(O)H]^{\ddagger}$ (aa) $TS2_e$: $[BrCH_2O + O_2 \rightarrow BrC(O)H + HO_2]^{\ddagger}$

Figure 2. Structures of the atmospheric degradation of bromoethane.

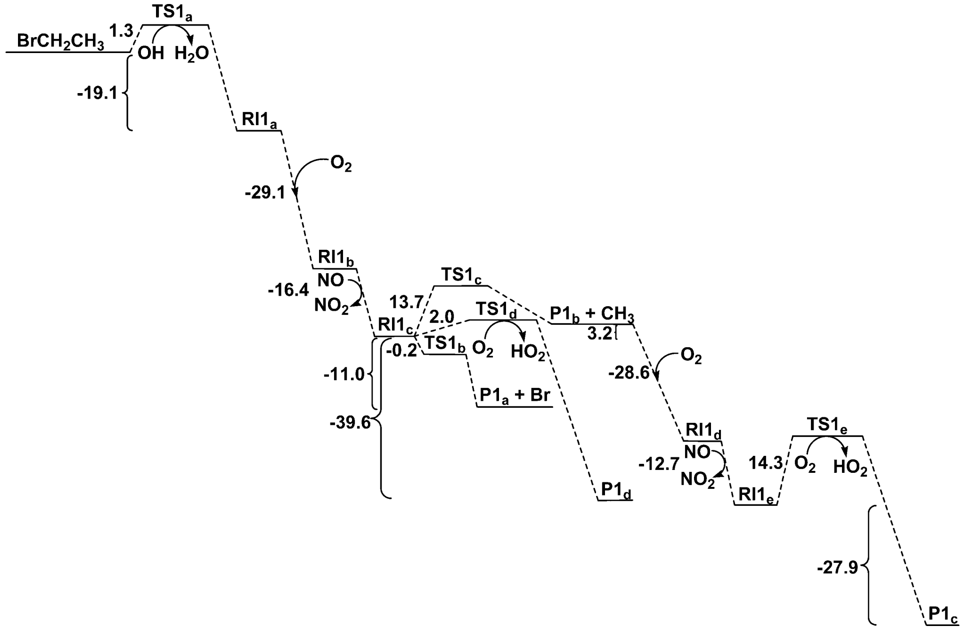

Figure 3. Potential energy surface for the hydrogen abstraction from the α carbon during the atmospheric degradation of bromoethane using CCSD(T)/6-311++G(2df,2p)//MP2/6-31G(d) level of theory.

2m). As shown in Figure 2m, the new CO bond has a length of 1.384 Å and the C−H bond has increased to 1.100 Å. The angles change as well, where the H−C−O angle is 108.0° and the C−C−Br angle is 109.5°. The $BrCH_2CH_2O$, like the $BrCHOCH_3$ alkoxy radical from the first pathway, undergoes either a unimolecular decomposition or oxidation with O_2. A formaldehyde molecule and a $BrCH_2$ (Figure 2n) radical are produced when $BrCH_2CH_2O$ undergoes a C−C bond fission, producing $BrCH_2$ and formaldehyde. It can be observed that $BrCH_2$ has a BrCH angle value of 116.7° and C−Br and C−H bond lengths of 1.863 and 1.079 Å, respectively. The oxidation of the brominated radical by molecular oxygen will give rise to $BrCH_2O_2$ (Figure 2o). This newly formed peroxy radical is reduced by NO, thus producing $BrCH_2O$ (shown in Figure 2p). This alkoxy radical can react via two different pathways. One pathway is through a C−Br bond fission that produces Br and formaldehyde. On the other hand, the oxidation of $BrCH_2O$ will form BrC(O)H. Oxidation of the $BrCH_2CH_2O$ radical takes place when it reacts with an O_2 molecule, producing HO_2 and $BrCH_2C(O)H$(Figure 2q).

3.1.2. Energetics of the Species Involved in the Atmospheric Degradation of Bromoethane. The complete atmospheric degradation mechanism of bromoethane is shown in Figure 1. The total energies of all the species involved in the present study, as well as the frequencies, are included in Tables 1 and 2, respectively. A list of all the calculated enthalpies of the reactions (ΔH_r), as well as the activation energy (E_a) barriers involved in the mechanism, are summarized in Tables 3 and 4. All the values reported in the potential energy surfaces (PESs) were calculated at the CCSD(T)/6-311++G(2df,2p)//MP2/6-31G(d) level of theory.

The energetics diagram for pathway 1 containing the calculated enthalpies of reaction and activation energy barriers is shown in Figure 3. This first pathway corresponds to the oxidation process that results from the H abstraction from the carbon α to the bromine. The hydrogen abstraction by OH radical requires overcoming an activation energy barrier of 1.3 kcal/mol. The enthalpy of reaction for the H abstraction is predicted to be −19.1 kcal/mol. The transition state corresponds to a first-order saddle-point identified by an imaginary frequency representing the C−H−O vibration at 2302 cm^{-1}. The newly formed radical, $BrCHCH_3$, undergoes oxidation via reaction with O_2 with a heat of reaction of −29.1 kcal/mol. The oxidation product, $BrCHO_2CH_3$, reacts with with the NO scavenger where the O−O bond breaks and another N−O bond formed. This has a ΔH_r of −16.4 kcal/mol.

The alkoxy radical formed, $BrCHOCH_3$, can participate in the following reaction channels:

$$BrCHOCH_3 \rightarrow Br + HC(O)CH_3 \tag{2}$$

$$BrCHOCH_3 \rightarrow BrC(O)H + CH_3 \tag{3}$$

$$BrCHOCH_3 + O_2 \rightarrow BrC(O)CH_3 + HO_2 \tag{4}$$

Reaction 2 is unimolecular release of Br atoms and shows a bond-breaking and bond-forming process in which the C−Br bond is broken and a C=O bond is formed. This fragmentation has a heat of reaction and a barrier height of −11.0 and −0.2 kcal/mol, respectively.

TABLE 1: Total Energies (hartrees) of the Reactants, Reactive Intermediates (RI), Products (P), and Transition States (TS) of the Atmospheric Degradation of Bromoethane

species	MP2/6-31G(d)[a]	CCSD(T)/6-311G(2d,2p)[a]	CCSD(T)/6-311++G(2df,2p)[a]
$BrCH_2CH_3$	−2648.883 46	−2651.485 02	−2651.546 50
OH	−75.514 69	−75.599 53	−75.624 91
H_2O	−76.177 76	−76.277 20	−76.306 62
O_2	−149.951 10	−150.067 77	−150.116 10
NO	−129.555 59	−129.658 08	−129.701 22
NO_2	−204.558 51	−204.707 84	−204.780 43
Br	−2569.981 46	−2572.470 43	−2572.504 08
HO_2	−150.487 97	−150.638 37	−150.689 05
Pathway 1			
$BrCHCH_3$	−2648.242 08	−2650.833 60	−2650.895 30
$BrCHO_2CH_3$	−2798.227 14	−2800.943 74	−2801.057 73
$BrCHOCH_3$	−2723.263 77	−2725.916 95	−2726.004 61
$HC(O)CH_3$	−153.301 97	−153.465 51	−153.518 13
$BrC(O)CH_3$	−2722.777 84	−2725.406 60	−2725.494 69
CH_3	−39.642 49	−39.713 47	−39.725 30
BrC(O)H	−2683.619 44	−2686.199 10	−2686.274 26
CH_3O_2	−189.623 53	−189.822 31	−189.886 94
CH_3O	−114.654 66	−114.789 28	−114.828 00
HC(O)H	−114.147 66	−114.260 24	−114.299 48
Pathway 2			
$BrCH_2CH_2$	−2648.240 35	−2650.831 90	−2650.893 52
$BrCH_2CH_2O_2$	−2798.224 13	−2800.942 01	−2801.055 70
$BrCH_2CH_2O$	−2723.256 28	−2725.909 94	−2725.997 84
$BrCH_2C(O)H$	−2722.753 15	−2725.383 97	−2725.473 13
$BrCH_2$	−2609.093 60	−2611.635 11	−2611.683 90
$BrCH_2O_2$	−2759.073 06	−2761.740 29	−2761.841 82
$BrCH_2O$	−2684.112 96	−2686.716 15	−2686.791 18

Transition States	MP2/6-31G(d)[a]	CCSD(T)/6-311G(2d,2p)[a]	CCSD(T)/6-311++G(2df,2p)[a]
Pathway 1			
$[BrCH_2CH_3 + OH \rightarrow BrCHCH_3 + H_2O]$	−2724.386 16	−2727.080 42	−2727.169 30
$[BrCHOCH_3 + O_2 \rightarrow BrC(O)CH_3 + HO_2]$	−2873.207 31	−2875.980 16	−2876.117 52
$[BrCHOCH_3 \rightarrow BrC(O)H + CH_3]$	−2723.234 52	−2725.894 90	−2725.982 76
$[BrCHOCH_3 \rightarrow Br + HC(O)CH_3]$	−2723.255 16	−2725.916 49	−2726.004 92
$[CH_3O + O_2 \rightarrow HC(O)H + HO_2]$	−264.542 08	−264.831 40	−264.921 34
Pathway 2			
$[BrCH_2CH_3 + OH \rightarrow BrCH_2CH_2 + H_2O]$	−2724.383 41	−2727.078 44	−2727.167 04
$[BrCH_2CH_2O + O_2 \rightarrow BrCH_2C(O)H + HO_2]$	−2873.191 72	−2875.967 42	−2876.105 50
$[BrCH_2CH_2O \rightarrow BrCH_2 + HC(O)H]$	−2723.215 02	−2725.880 56	−2725.969 88
$[BrCH_2O + O_2 \rightarrow BrC(O)H + HO_2]$	−2834.052 94	−2836.778 07	−2836.902 84
$[BrCH_2O \rightarrow Br + HC(O)H]$	−2684.098 93	−2686.712 26	−2686.787 62

[a] Corrected with ZPE.

Reaction 3 is another unimolecular dissociation reaction in which the C−C bond is broken and a C=O bond is formed with an activation energy of 13.7 kcal/mol. This slightly endothermic reaction has a calculated reaction enthalpy of 3.2 kcal/mol. The fragmentation process represented in reaction 3 produces a CH_3 radical that is further oxidized by O_2 molecule, having a ΔH_r of −28.6 kcal/mol. The formed organic peroxy radical, CH_3O_2, reacts with NO, breaking the O−O bond to form NO_2. This bond-breaking and bond-forming process is −12.7 kcal/mol exothermic. The newly formed alkoxy radical, CH_3O, can react with an O_2 molecule, forming the HC(O)H and HO_2 by overcoming a barrier height of 14.3 kcal/mol. This reaction is exothermic by −27.9 kcal/mol. The first-order saddle point representing the C−H−O vibration is found to be at 3744 cm^{-1}.

On the other hand, reaction 4 represents the alkoxy radical reaction with O_2. In this oxidation process, a hydrogen is abstracted from the alkoxy radical by the O_2 molecule with an activation energy and a heat of reaction of 2.0 and −39.6 kcal/mol, respectively. Through vibrational frequency analysis, the first-order saddle points representing the C−Br, C−C, and C−H−O vibrations for reactions 2, 3, and 4 are found to be at 609, 649, and 960 cm^{-1}, respectively.

Figure 4 is the energetics diagram containing the calculated enthalpies of reaction and activation energy barriers for Pathway 2. This second pathway corresponds to the oxidation process that results from the H abstraction from the carbon β to the bromine. The calculated barrier height for the abstraction of the β hydrogen is predicted to be 2.7 kcal/mol. This reaction has a ΔH_r of −18.0 kcal/mol. One negative frequency representing the C−H−O vibration at 2132 cm^{-1} indicated the transition state is a first-order saddle point. After the H abstraction, the radical formed reacts with an O_2 molecule to form $BrCH_2CH_2O_2$. This step has a reaction enthalpy of −28.9 kcal/mol. Immediately after the peroxy radical is formed, NO reacts with $BrCH_2CH_2O_2$ to form $BrCH_2CH_2O$ and NO_2 by breaking a C−O bond. This bond-breaking and bond-formation step has a heat of reaction of −13.4 kcal/mol.

The newly formed alkoxy radical $BrCH_2CH_2O$ from pathway 2 can participate in the following reaction processes:

$$BrCH_2CH_2O \rightarrow BrCH_2 + HC(O)H \qquad (5)$$

$$BrCH_2CH_2O + O_2 \rightarrow BrCH_2C(O)H + HO_2 \qquad (6)$$

Reaction 5 represents the C−C bond breakage and the C=O bond formation with an activation barrier of 17.5 kcal/mol and a ΔH_r of 9.1 kcal/mol. The $BrCH_2$ radical formed reacts with an O_2 molecule with an enthalpy of reaction of −26.2 kcal/mol. The newly formed $BrCH_2O_2$ will react with the NO

TABLE 2: Vibrational Frequencies (cm^{-1}) of the Reactants, Products, and Transition States of the Atmospheric Degradation of Bromoethane

species	vibrational frequencies
$BrCH_2CH_3$	3246, 3220, 3202, 3169, 3112, 1563, 1551, 1550, 1473, 1333, 1314, 1123, 1074, 1014, 796, 596, 299, 279
OH	3740
H_2O	3918, 3776, 1736
O_2	1413
NO	3895
NO_2	2290, 1382, 753
HO_2	3606, 1477, 1237
	Pathway 1
$BrCHCH_3$	3294, 3206, 3166, 3080, 1548, 1532, 1469, 1328, 1155, 1056, 1042, 647, 472, 306, 182
$BrCHO_2CH_3$	3235, 3224, 3210, 3124, 1549, 1542, 1465, 1378, 1302, 1249, 1153, 1116, 1047, 879, 713, 450, 393, 296, 280, 249, 79
$BrCHOCH_3$	3246, 3232, 3129, 3107, 1551, 1542, 1454, 1295, 1251, 1138, 1037, 999, 935, 594, 343, 324, 300, 257
$HC(O)CH_3$	3235, 3185, 3105, 2990, 1801, 1535, 1527, 1468, 1440, 1170, 1168, 926, 800, 515, 152
$BrC(O)CH_3$	3240, 3222, 3124, 1894, 1525, 1524, 1443, 1143, 1076, 985, 573, 500, 336, 310, 167
BrC(O)H	3146, 1822, 1348, 925, 652, 358
CH_3	3410, 3410, 3221, 1481, 1481, 405
CH_3O_2	3263, 3254, 3138, 1551, 1540, 1502, 1276, 1221, 1172, 965, 507, 139
CH_3O	3168, 3136, 3051, 1583, 1484, 1466, 1143, 1001, 838
HC(O)H	3010, 3081, 1793, 1297, 1585, 1214
	Pathway 2
$BrCH_2CH_2$	3364, 3264, 3249, 3187, 1560, 1522, 1300, 1253, 1134, 1058, 791, 672, 539, 276, 265
$BrCH_2CH_2O_2$	3264, 3236, 3180, 3160, 1546, 1543, 1420, 1341, 1288, 1265, 1227, 1111, 1051, 949, 799, 718, 535, 300, 219, 117, 97
$BrCH_2CH_2O$	3254, 3175, 3104, 3056, 1542, 1483, 1412, 1320, 1275, 1111, 1105, 1068, 843, 711, 529, 362, 223, 131
$BrCH_2C(O)H$	3251, 3157, 3038, 1787, 1509, 1445, 1271, 1201, 1090, 1005, 819, 658, 444, 270, 68
$BrCH_2$	3414, 3260, 1457, 975, 712, 428
$BrCH_2O_2$	3280, 3182, 1529, 1363, 1231, 1227, 995, 932, 754, 396, 246, 49
$BrCH_2O$	3166, 3091, 1436, 1318, 1128, 1067, 673, 623, 330
	Transition States
	Pathway 1
$[BrCH_2CH_3 + OH \rightarrow BrCHCH_3 + H_2O]^{\ddagger}$	3724, 3226, 3209, 3201, 3112, 1549, 1543, 1485, 1469, 1338, 1262, 1148, 1127, 1027, 835, 806, 652, 595, 302, 255, 194, 106, 83, 2302i
$[BrCHOCH_3 + O_2 \rightarrow BrC(O)CH_3 + HO_2]^{\ddagger}$	3246, 3225, 3123, 1999, 1941, 1545, 1533, 1479, 1435, 1228, 1114, 1028, 980, 768, 647, 532, 381, 346, 300, 256, 236, 203, 89, 960i
$[BrCHOCH_3 \rightarrow BrC(O)H + CH_3]^{\ddagger}$	3373, 3359, 3182, 3082, 1805, 1495, 1479, 1288, 1137, 990, 737, 694, 579, 395, 302, 219, 199, 649i
$[BrCHOCH_3 \rightarrow Br + HC(O)CH_3]^{\ddagger}$	3250, 3208, 3113, 3098, 1548, 1534, 1492, 1450, 1352, 1174, 1051, 940, 878, 497, 288, 247, 234, 609i
$[CH_3O + O_2 \rightarrow HC(O)H + HO_2]^{\ddagger}$	3065, 2951, 1822, 1601, 1478, 1424, 1257, 1166, 1004, 606, 411, 242, 123, 51, 3744i
	Pathway 2
$[BrCH_2CH_3 + OH \rightarrow BrCH_2CH_2 + H_2O]^{\ddagger}$	3727, 3265, 3247, 3182, 3170, 1549, 1528, 1497, 1342, 1319, 1289, 1134, 1097, 1052, 875, 807, 724, 595, 403, 237, 119, 73, 62, 2132i
$[BrCH_2CH_2O + O_2 \rightarrow BrCH_2C(O)H + HO_2]^{\ddagger}$	3245, 3167, 3030, 1812, 1782, 1554, 1522, 1403, 1369, 1291, 1204, 1069, 1026, 835, 737, 709, 590, 420, 346, 287, 188, 155, 66, 1856i
$[BrCH_2CH_2O \rightarrow BrCH_2 + HC(O)H]^{\ddagger}$	3373, 3236, 3057, 2984, 1710, 1557, 1463, 1293, 1210, 1014, 955, 772, 668, 582, 300, 169, 108, 736i
$[BrCH_2O + O_2 \rightarrow BrC(O)H + HO_2]^{\ddagger}$	3292, 3165, 2056, 1763, 1443, 1394, 1009, 994, 654, 539, 346, 264, 74, 58, 1522i
$[BrCH_2O \rightarrow Br + HC(O)H]^{\ddagger}$	3180, 3084, 1630, 1414, 1257, 1008, 778, 244, 623i

scavenger to break an O−O bond and form another N−O bond. This bond-breaking and bond-formation step has a reaction enthalpy of −17.9 kcal/mol. The alkoxy radical formed, $BrCH_2O$, has two reaction routes. The first is the dissociation of the alkoxy radical to release a Br atom and HC(O)H, which has a heat of reaction of −7.8 kcal/mol and an activation energy barrier of 2.2 kcal/mol. On the other hand, the $BrCH_2O$ alkoxy radical can react with an O_2 molecule to form BrC(O)H and HO_2. The energy barrier height that the reaction has to overcome in order to take place is 2.8 kcal/mol. The calculated reaction enthalpy is −35.2 kcal/mol.

Reaction 6, involving the reaction of the $BrCH_2CH_2O$ radical with an O_2 molecule, has a reaction enthalpy −30.3 kcal/mol. The activation energy barrier that it has to overcome is only 5.3 kcal/mol, indicating that this is the most favorable route to end products from pathway 2.

3.2. Atmospheric Implications. The atmospheric oxidation mechanism of bromoethane that results from abstractions of both

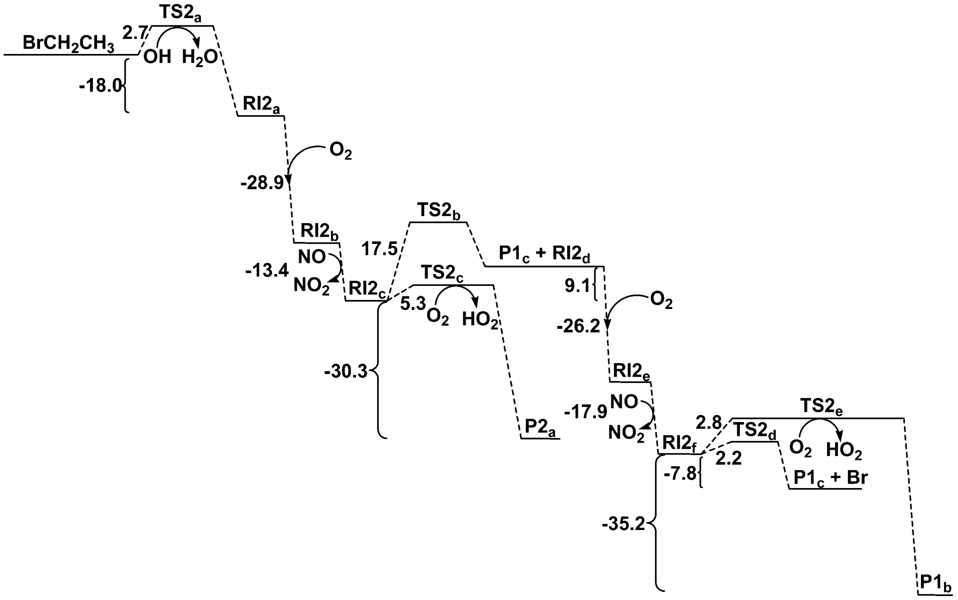

Figure 4. Potential energy surface for the hydrogen abstraction from the β carbon during the atmospheric degradation of bromoethane using CCSD(T)/6-311++G(2df,2p)//MP2/6-31G(d) level of theory.

TABLE 3: Heats of Formation (ΔH_f) in kcal/mol for the Reactions Involved in the Atmospheric Degradation of Bromoethane

reactions	MP2/6-31G(d)[a]	CCSD(T)/6-311G(2d,2p)[a]	CCSD(T)/6-311++G(2df,2p)[a]
	Pathway 1		
$BrCH_2CH_3 + OH \rightarrow BrCHCH_3 + H_2O$	−13.6	−16.5	−19.1
$BrCHCH_3 + O_2 \rightarrow BrCHO_2CH_3$	−21.3	−26.6	−29.1
$BrCHO_2CH_3 + NO \rightarrow BrCHOCH_3 + NO_2$	−24.8	−14.4	−16.4
$BrCHOCH_3 \rightarrow Br + HC(O)CH_3$	−12.3	−11.9	−11.0
$BrCHOCH_3 + O_2 \rightarrow BrC(O)CH_3 + HO_2$	−32.0	−37.8	−39.6
$BrCHOCH_3 \rightarrow BrC(O)H + CH_3$	1.2	2.8	3.2
$CH_3 + O_2 \rightarrow CH_3O_2$	−18.8	−25.8	−28.6
$CH_3O_2 + NO \rightarrow CH_3O + NO_2$	−21.4	−10.5	−12.7
$CH_3O + O_2 \rightarrow HC(O)H + HO_2$	−18.7	−26.1	−27.9
	Pathway 2		
$BrCH_2CH_3 + OH \rightarrow BrCH_2CH_2 + H_2O$	−12.5	−15.4	−18.0
$BrCH_2CH_2 + O_2 \rightarrow BrCH_2CH_2O_2$	−20.5	−26.6	−28.9
$BrCH_2CH_2O_2 + NO \rightarrow BrCH_2CH_2O + NO_2$	−22.0	−11.1	−13.4
$BrCH_2CH_2O + O_2 \rightarrow BrCH_2C(O)H + HO_2$	−21.2	−28.0	−30.3
$BrCH_2CH_2O \rightarrow BrCH_2 + HC(O)H$	9.4	9.2	9.1
$BrCH_2 + O_2 \rightarrow BrCH_2O_2$	−17.8	−23.5	−26.2
$BrCH_2O_2 + NO \rightarrow BrCH_2O + NO_2$	−26.9	−16.1	−17.9
$BrCH_2O \rightarrow Br + HC(O)H$	−10.1	−9.1	−7.8
$BrCH_2O + O_2 \rightarrow BrC(O)H + HO_2$	−27.2	−33.6	−35.2

[a] Corrected with ZPE.

TABLE 4: Activation Energies (E_a) in kcal/mol for the Transition States Involved in the Atmospheric Degradation of Bromoethane

transition states	MP2/6-31G(d)[a]	CCSD(T)/6-311G(2d,2p)[a]	CCSD(T)/6-311++G(2df,2p)[a]
	Pathway 1		
$[BrCH_2CH_3 + OH \rightarrow BrCHCH_3 + H_2O]$	7.5	2.6	1.3
$[BrCHOCH_3 + O_2 \rightarrow BrC(O)CH_3 + HO_2]$	4.7	2.9	2.0
$[BrCHOCH_3 \rightarrow BrC(O)H + CH_3]$	18.4	13.8	13.7
$[BrCHOCH_3 \rightarrow Br + HC(O)CH_3]$	5.4	0.3	−0.2
$[CH_3O + O_2 \rightarrow HC(O)H + HO_2]$	40.0	16.1	14.3
	Pathway 2		
$[BrCH_2CH_3 + OH \rightarrow BrCH_2CH_2 + H_2O]$	9.2	3.8	2.7
$[BrCH_2CH_2O + O_2 \rightarrow BrCH_2C(O)H + HO_2]$	9.8	6.5	5.3
$[BrCH_2CH_2O \rightarrow BrCH_2 + HC(O)H]$	25.9	18.4	17.5
$[BrCH_2O + O_2 \rightarrow BrC(O)H + HO_2]$	7.0	3.7	2.8
$[BrCH_2O \rightarrow Br + HC(O)H]$	8.8	2.4	2.2

[a] Corrected with ZPE.

the α and β carbons has been assessed in this work. Abstracting the hydrogen from the α carbon is considered the most favorable pathway. This is because it has to overcome the smallest activation energy barrier of the two pathways, 1.3 kcal/mol.

By means of this atmospheric oxidation route, the possible products that could result from the degradation of bromoethane are as follows. The energetically favored α abstraction can produce the following end products: Br, $BrC(O)CH_3$, $BrC(O)H$,

$HC(O)CH_3$, and HC(O)H. For the secondary H abstraction, the possible end products that could be observed are Br, $BrCH_2C(O)H$, BrC(O)H, and two HC(O)H. Note that each of the pathways produces Br. An extensive literature search has shown that not many studies have been performed to characterize the species $BrC(O)CH_3$ and $BrCH_2C(O)H$.

As previously mentioned, Orlando and co-workers[30] performed the most extensive experimental studies on bromoethane. Briefly, oxidation of bromoethane was initiated by reaction with Cl over a range of temperatures (220−298 K) and O_2 partial pressures (20−650 Torr). Studies were performed in both the presence and absence of NO_x. For this discussion, the authors will focus on the experimental studies performed in the presence of NO_x, since the calculations described in this article are performed considering the presence of NO. The experimental findings suggest that 70−80% of the hydrogen abstraction occurs on the α carbon, which is in agreement with our findings. After forming the alkoxy radical, the experimental studies confirm the calculations described in this article by $HC(O)CH_3$ as the primary product of the α abstraction. Therefore, Br elimination dominates, as previously observed for α-brominated alkoxy radicals.[30,35,48] According to our model, other species that could be observed as part of the α abstraction are BrC(O)H, HC(O)H, and $BrC(O)CH_3$. Under the experimental conditions in the presence of NO_x, Orlando and co-workers did not observe the presence of any of the above-mentioned compounds. In the NO_x-free environment studies, the group observed HC(O)H and $BrC(O)CH_3$ but described alternate routes to describe their formation. Bierbach and co-workers[31] described their observation of $BrC(O)CH_3$ as a reaction of the alkoxy radical $BrCHOCH_3$ with O_2 in their study of the oxidation of *trans*-2-butene initiated by Br. According to the findings of the experimental studies by Orlando and co-workers,[30] it is shown that $BrC(O)CH_3$ is obtained via reactions among $BrCHO_2CH_3$ radicals instead of the alkoxy radicals reacting with O_2. Even though Orlando and co-workers[30] do not mention products from the abstraction as part of their studies in the NO_x experiments, they identify $BrCH_2C(O)H$ in the product spectra, which from our findings is the most favorable product of this minor channel.

Acknowledgment. The authors gratefully acknowledge the financial support given by the U.S. Department of Energy, Global Change Education Program Graduate Research Environmental Fellowship to Mónica Martínez-Avilés.

Supporting Information Available: Cartesian coordinates at the MP2/6-31G(d) level of theory for the species involved in the atmospheric degradation of bromoethane. This material is available free of charge via the Internet at http://pubs.acs.org.

References and Notes

(1) Yu, X.; Ichihara, G.; Kitoh, J.; Xie, Z.; Shibata, E.; Kamijima, M.; Asaeda, N.; Takeuchi, Y. *J. Occup. Health* **1998**, *40*, 234.

(2) Wuebbles, D. J.; Jain, A. K.; Patten, K. O.; Connell, P. S. *Atmos. Environ.* **1997**, *32*, 107.

(3) Ko, M. K. W.; Poulet, G. *Scientific Assessment of Ozone Depletion: 2002*; Global Ozone Research and Monitoring Project, Report No. 47; World Meteorological Organization: Geneva, Switzerland, 2003.

(4) Yung, Y. L.; Pinto, J. P.; Watson, R. T.; Sander, S. P. *J. Atmos. Sci.* **1980**, *37*, 339.

(5) Dixon, D. A.; de Jong, W. A.; Peterson, K. A.; Francisco, J. S. *J. Phys. Chem. A* **2002**, *106*, 4725.

(6) Scientific Assessment of Stratospheric Ozone; 1989; Global Ozone Research and Monitoring Project, Report No. 20; World Meteorological Organization: Geneva, Switzerland, 1990.

(7) Daniel, J. S.; Solomon, S.; Portmann, R. W.; Garcia, R. R. *J. Geophys. Res.* **1999**, *104*, 23871.

(8) Kamboures, M. A.; Hansen, J. C.; Francisco, J. S. *Chem. Phys. Lett.* **2002**, *353*, 335.

(9) Anderson, J. G.; Brune, W. H.; Lloyd, S. A.; Toohey, D. W.; Sander, S. P.; Starr, W. L.; Loewenstein, M.; Podolske, J. R. *J. Geophys. Res.* **1989**, *94*, 11480.

(10) Bucher, J. R.; Morgan, D. L.; Adkins, B., J.; Travlos, G. S.; Davis, B. J.; Morris, R.; Elwell, M. R. *Toxicol. Appl. Pharmacol.* **1995**, *130*, 169.

(11) Class, T.; Kohnle, R.; Ballschmiter, K. *Chemosphere* **1986**, *15*, 429.

(12) Greenberg, J. P.; Guenther, A. B.; Turnipseed, A. *Environ. Chem.* **2005**, *2*, 291.

(13) Low, J. C.; Wang, N. Y.; Williams, J.; Cicerone, R. J. *J. Geophys. Res.* **2003**, *108*, ACH7.

(14) Carpenter, L. J.; Sturges, W. T.; Penkett, S. A.; Liss, P. S.; Alicke, B.; Hebestreit, K.; Platt, U. *J. Geophys. Res.* **1999**, *104*, 1679.

(15) Jordan, A.; Harnisch, J.; Borchers, R.; Guern, F. L.; Shinohara, H. *Environ. Sci. Technol.* **2000**, *34*, 1122.

(16) Gould, J. P.; Ramsay, R. E.; Giabbai, M.; Pohland, F. G. Formation of Volatile Haloorganic Compounds in the Chlorination of Municipal Landfill Leachates. In *Water Chlorination: Environmental Impact and Health Effects*; Jolley, R. L., Brungs, W. A., Cotruvo, J. A., Cumming, R. B., Mattice, J. S., Jacobs, V. A., Eds.; Ann Arbor Science Publishers: Ann Arbor, MI, 1983; Vol. 4, p 525.

(17) Brown, K. W.; Donnelly, K. C. *Hazard. Waste Hazard. Mater.* **1988**, *5*, 1.

(18) Levy, H., II. *Planet. Space Sci.* **1972**, *20*, 919.

(19) Matthews, J.; Sinha, A.; Francisco, J. S. *Proc. Natl. Acad. Sci.* **2005**, *102*, 7449.

(20) Atkinson, R. *Chem. Rev.* **1986**, *86*, 69.

(21) Atkinson, R. *Int. J. Chem. Kinet.* **1987**, *19*, 799.

(22) Atkinson, R.; Carter, W. P. L. *Chem. Rev.* **1984**, *84*, 437.

(23) Atkinson, R. *Int. J. Chem. Kinet.* **1986**, *18*, 555.

(24) Finlayson-Pitts, B. J.; Pitts, J. N. *Atmospheric Chemistry: Fundamentals and Experimental Techniques*; John Wiley and Sons, Inc.: New York, 1986.

(25) Qiu, L. X.; Shi, S. H.; Xing, S. B.; Chen, X. G. *J. Phys. Chem.* **1992**, *96*, 685.

(26) Xing, S.-B.; Shi, S.-H.; Qiu, L.-X. *Int. J. Chem. Kinet.* **1992**, *24*, 1.

(27) Herndon, S. C.; Gierczak, T.; Talukdar, R. K.; Ravishankara, A. R. *Phys. Chem. Chem. Phys.* **2001**, *3*, 4529.

(28) Donaghy, T.; Shanahan, I.; Hande, M.; Fitzpatrick, S. *Int. J. Chem. Kinet.* **1993**, *25*, 273.

(29) Hazardous Substances Data Bank (HSDB); SilverPlatter International Chem-Bank, U.S. National Library of Medicine: Bethesda, MD, 2000.

(30) Orlando, J. J.; Tyndall, G. S. *J. Phys. Chem. A* **2002**, *106*, 312.

(31) Bierbach, A.; Barnes, I.; Becker, K. H. *Tellus B* **1997**, *49*, 566.

(32) Bilde, M.; Orlando, J. J.; Tyndall, G. S.; Wallington, T. J.; Hurley, M. D.; Kaiser, E. W. *J. Phys. Chem. A* **1999**, *103*, 3963.

(33) Bilde, M.; Sehested, J.; Nielsen, O. J.; Wallington, T. J. *J. Phys. Chem. A* **1997**, *101*, 5477.

(34) Catoire, V.; Lesclaux, R.; Lightfoot, P. D.; Rayez, M. T. *J. Phys. Chem.* **1994**, *98*, 2889.

(35) Chen, J.; Catoire, V.; Niki, H. *Chem. Phys. Lett.* **1995**, *245*, 519.

(36) Shi, J.; Wallington, T. J.; Kaiser, E. W. *J. Phys. Chem.* **1993**, *97*, 6184.

(37) Maricq, M. M.; Shi, J.; Szente, J. J.; Rimai, L.; Kaiser, E. W. *J. Phys. Chem.* **1993**, *97*, 9686.

(38) Kaiser, E. W.; Wallington, T. J. *J. Phys. Chem.* **1994**, *98*, 5679.

(39) Kaiser, E. W.; Wallington, T. J. *J. Phys. Chem.* **1995**, *99*, 8669.

(40) Wallington, T. J.; Bilde, M.; Mogelberg, T. E.; Sehested, J.; Nielsen, O. J. *J. Phys. Chem.* **1996**, *100*, 5751.

(41) Wallington, T. J.; Hurley, M. D.; Schneider, W. F. *Chem. Phys. Lett.* **1996**, *251*, 164.

(42) Wallington, T. J.; Orlando, J. J.; Tyndall, G. S. *J. Phys. Chem.* **1995**, *99*, 9437.

(43) Wu, F.; Carr, R. W. *Chem. Phys. Lett.* **1999**, *305*, 44.

(44) Wu, F.; Carr, R. W. *J. Phys. Chem. A* **2001**, *105*, 1423.

(45) Wang, B.; Hou, H.; Gu, Y. *J. Phys. Chem. A* **1999**, *103*, 2060.

(46) Platz, J.; Nielsen, O. J.; Sehested, J.; Wallington, T. J. *J. Phys. Chem.* **1995**, *99*, 6570.

(47) Villenave, E.; Lesclaux, R. *Chem. Phys. Lett.* **1995**, *236*, 376.

(48) Orlando, J. J.; Tyndall, G. S.; Wallington, T. J. *J. Phys. Chem.* **1996**, *100*, 7026.

(49) Hou, H.; Wang, B.; Gu, Y. *J. Phys. Chem. A* **2000**, *104*, 1570.

(50) Frisch, M. J.; Trucks, G. W.; Schlegel, H. B.; Scuseria, G. E.; Robb, M. A.; Cheeseman, J. R.; J. A. Montgomery, J.; Vreven, T.; Kudin, K. N.; Burant, J. C.; Millam, J. M.; Iyengar, S. S.; Tomasi, J.; Barone, V.;

Mennucci, B.; Cossi, M.; Scalmani, G.; Rega, N.; Petersson, G. A.; Nakatsuji, H.; Hada, M.; Ehara, M.; Toyota, K.; Fukuda, R.; Hasegawa, J.; Ishida, M.; Nakajima, T.; Honda, Y.; Kitao, O.; Nakai, H.; Klene, M.; Li, X.; Knox, J. E.; Hratchian, H. P.; Cross, J. B.; Adamo, C.; Jaramillo, J.; Gomperts, R.; Stratmann, R. E.; Yazyev, O.; Austin, A. J.; Cammi, R.; Pomelli, C.; Ochterski, J. W.; Ayala, P. Y.; Morokuma, K.; Voth, G. A.; Salvador, P.; Dannenberg, J. J.; Zakrzewski, V. G.; Dapprich, S.; Daniels, A. D.; Strain, M. C.; Farkas, O.; Malick, D. K.; Rabuck, A. D.; Raghavachari, K.; Foresman, J. B.; Ortiz, J. V.; Cui, Q.; Baboul, A. G.; Clifford, S.; Cioslowski, J.; Stefanov, B. B.; Liu, G.; Liashenko, A.; Piskorz, P.; Komaromi, I.; Martin, R. L.; Fox, D. J.; Keith, T.; Al-Laham, M. A.; Peng, C. Y.; Nanayakkara, A.; Challacombe, M.; Gill, P. M. W.; Johnson, B.; Chen, W.; Wong, M. W.; Gonzalez, C.; Pople, J. A. *Gaussian 03*, revision B.03; Gaussian, Inc.: Pittsburgh, PA, 2003.

(51) Moller, C.; Plesset, M. S. *Phys. Rev.* **1934**, *46*, 618.